AAPS PharmSciTech, Vol. 13, No. 3, September 2012 (© 2012)
DOI: 10.1208/s12249-012-9796-1

Research Article

Design of Experiments-Based Monitoring of Critical Quality Attributes for the Spray-Drying Process of Insulin by NIR Spectroscopy

Morten Jonas Maltesen,[1,2,3] Marco van de Weert,[1] and Holger Grohganz[1]

Received 29 November 2011; accepted 20 April 2012; published online 15 May 2012

Abstract. Moisture content and aerodynamic particle size are critical quality attributes for spray-dried protein formulations. In this study, spray-dried insulin powders intended for pulmonary delivery were produced applying design of experiments methodology. Near infrared spectroscopy (NIR) in combination with preprocessing and multivariate analysis in the form of partial least squares projections to latent structures (PLS) were used to correlate the spectral data with moisture content and aerodynamic particle size measured by a time of flight principle. PLS models predicting the moisture content were based on the chemical information of the water molecules in the NIR spectrum. Models yielded prediction errors (RMSEP) between 0.39% and 0.48% with thermal gravimetric analysis used as reference method. The PLS models predicting the aerodynamic particle size were based on baseline offset in the NIR spectra and yielded prediction errors between 0.27 and 0.48 μm. The morphology of the spray-dried particles had a significant impact on the predictive ability of the models. Good predictive models could be obtained for spherical particles with a calibration error (RMSECV) of 0.22 μm, whereas wrinkled particles resulted in much less robust models with a Q^2 of 0.69. Based on the results in this study, NIR is a suitable tool for process analysis of the spray-drying process and for control of moisture content and particle size, in particular for smooth and spherical particles.

KEY WORDS: moisture content; multivariate analysis; NIR; particle size; spray-drying.

INTRODUCTION

The process analytical technology (PAT) initiative and quality by design approach to product design and production, as described in the ICH Q8–Q10, have recently been incorporated by the European Medicines Agency and the US Food and Drug Administration to ensure higher-quality products and faster development (1–3). Basically, the framework aims at a better process understanding and process design to ensure quality. The first step is to define the desired target product profile (TPP), which refers to the characteristics ensuring efficacy and safety of the drug product. The TPP includes dosage form and administration route. The second step is identifying critical quality attributes (CQA), which are physical and chemical properties or characteristics important for the TPP and thus the quality of the final product. The limits of the CQAs define the product design space (4,5) which is preferably investigated applying a design of experiments (DoE) approach and analysed in real time. This is the core idea of the PAT framework (3). Near infrared (NIR) spectroscopy has traditionally been used as the preferred analytical method when incorporating the PAT initiative (6–8). The reasons for the success of NIR spectroscopy include the absence of sample preparation, fast analysis time, as well as noninvasive and nondestructive sample analysis (9,10). The application of multivariate data analysis is usually necessary to understand the highly complex process as well as for the spectral data analysis.

Proteins are labile molecules and stabilisation is often needed in order to obtain products with a suitable shelf life (11,12). The most common approach towards stabilising protein drugs is to remove the water from the formulation (13,14), often in the presence of specific excipients which prevent protein unfolding due to dehydration stress (15,16). Water tends to decrease the shelf life of proteins by increasing the molecular mobility of the protein, and acts as a reactant in several degradation pathways (14). Thus, the moisture content of the final drug product is a CQA referring to the protein stability. There is an increasing interest in understanding the solid-state properties of biopharmaceuticals where the final product is governed by complex interactions between protein, excipient and the process parameters of an applied process, such as spray drying.

For pulmonary delivery the particle size, particle size distribution and moisture content are important CQAs (17–19). Pulmonary delivery has been stated as an attractive alternative to the subcutaneous administration route used presently as the preferred administration route for proteins. The large surface area and a thin lung epithelium in the deep lungs make

[1] Department of Pharmaceutics and Analytical Chemistry, Faculty of Pharmaceutical Sciences, University of Copenhagen, Copenhagen, Denmark.
[2] Biopharma Application Development, Novozymes Biopharma A/S, Krogshoejvej 36, 2880 Bagsvaerd, Denmark.
[3] To whom correspondence should be addressed. (e-mail: mjom@novozymes.com)

the absorption of proteins easier compared with other noninvasive routes. The deposition of particles in the deep lungs is controlled by a number of parameters, with aerodynamic particle size being the most important. The aerodynamic particle size should be in the range of 1–5 μm for optimal delivery. In addition to deposition in the deep lungs, particle size is important for bioavailability and dose uniformity. Particles with the optimal aerodynamic particle size can be manufactured in several different ways, including milling and spray drying (17,20).

Spray drying is a popular manufacturing process for particles in general and has been used for several decades in the food industry (21). In the pharmaceutical industry, it has so far mainly been applied to producing particles intended for inhalation. Several companies have had spray-dried insulin in the pipeline as a drug candidate for the future, and the only approved systemic protein drug administered through the lungs was manufactured by spray drying (22). The spray-drying process is a one-step unit operation which is attractive from an economic perspective, but what makes it attractive in the field of pulmonary delivery is the unique control of particle size and particle size distribution of dried powders (18–20,23). By adjusting the process parameters in the spray-drying process, the particle size can be controlled and an aerodynamic particle size in the size range of 1–5 μm can be obtained (24,25). The concept of expressing particle size in one numerical descriptor is only valid for spherical particles, but many spray-dried formulations do not yield completely spherical particles. Instead, the aerodynamic particle size is used, which is defined as the diameter of a spherical particle of unit density having the same terminal velocity as the measured particle. Thus, the conversion between geometric particle size and aerodynamic particle size is dependent on both shape factor and particle density (26,27). Since the particle size is critical to the deposition in the lungs, and thereby the success of a solid formulation, controlling the particle size is important for a successful formulation.

In the NIR region, spray-dried powders both absorb and scatter light, resulting in spectra with overlapping bands, nonconstant baselines and varying offsets. The absorption bands are dominated by the overtones and combinations of functional groups, whereas scatter in the NIR region is caused by mismatched refractive indices at the interfaces in the sample and depends among other things on the particle size, morphology and density of the powders (28,29). Thus, for the measurement of chemical properties of solid materials, scatter is a complicating factor. *Vice versa*, absorbance bands constitute a complicating factor for the determination of physical properties of the solid. Several studies have investigated the particle size in various processes (6,8,28,30–33) and the moisture content of lyophilized sugars and proteins by NIR (7,8,30,34–36). However, NIR has seldom been applied to monitor the spray-drying process, and has rarely been used when proteins are the model system (37). In addition, NIR has so far not been correlated with aerodynamic particle size; however, this should be possible as both NIR scattering and aerodynamic particle size are related to geometric particle size, density and morphology. Furthermore the spray-drying process can yield particles with highly distinct morphologies which present a challenge for particle size analysis.

The objective of the present study is to utilize NIR as a PAT tool to address aerodynamic particle size and moisture content of spray-dried insulin intended for inhalation. DoE was used to choose process parameter settings for the production of spray-dried insulin particles with varying particle sizes and moisture contents. The moisture content was measured with thermogravimetric analysis (TGA) and the aerodynamic particle size was measured with a time of flight (TOF) principle. NIR spectra were correlated with the measured moisture content and particle size using partial least square projections to latent structures (PLS) in order to obtain prediction models. Furthermore, three different particle morphologies were obtained from the spray-drying process and the effect of these on the prediction power was evaluated.

MATERIALS AND METHODS

Materials

Biosynthetic human insulin containing two Zn atoms per hexamer was kindly supplied by Novo Nordisk A/S, Bagsvaerd, Denmark. All other chemicals were commercially available chemicals of analytical grade. Deionized water was filtered using a Millipore system (Millipore, Billerica, MA, USA) and used for all samples.

Sample Preparation

Insulin solutions were prepared by dissolving the insulin in a minimal volume of 0.2 M ice-cold hydrochloric acid resulting in a pH of approximately 2.5, which is below the isoelectric point of the insulin monomer (5.3) and hexamer (6.4) (38). After dissolution of the insulin, the pH was adjusted to 8.0 with 0.2 M ice-cold sodium hydroxide. The insulin concentration was determined from absorbance at 276 nm using a molar extinction coefficient of 6,200 M^{-1} cm^{-1} and adjusted to 5 mg/mL (0.8 mM), 30 mg/mL (5 mM) or 60 mg/mL (10 mM) with water.

DoE-Based Setup of Spray Drying

Spray drying was performed with a Büchi B-290 spray dryer (Büchi Labortechnik AG, Flawil, Switzerland) according to standard procedures (24). The humidity of the inlet drying air was controlled and kept below 20%. A two-fluid-nozzle design with nitrogen as atomising gas was used in a cocurrent mode. Spray-dried particles were separated from the drying air by a standard cyclone and manually transferred to glass vials immediately after production. The spray-dried powders were stored in vials at 5°C and at a relative humidity of 20%. A central composite face-centred design (CCF) designed in SAS-JMP (SAS Institute Inc., Cary, USA) was used to create a large design space for the investigated parameters: nozzle gas flow rate (N), feed flow rate (F), inlet drying air temperature (T_{in}), inlet drying air flow rate (A) and insulin concentration (I). The experimental design is explained in more detail in (24). In brief, N, F, T_{in}, A and I were included in the CCF design at three levels (Table I) utilizing 31 experiments. A two-level fractional factorial design (2^{5-1} design) consisting of 16 experiments was combined with 10 star points with a high and low level for each parameter, and 5

Table I. Process and Formulation Parameters

Parameter		Low level	Centre level	High level
Nozzle gas flow rate (L/min)	N	7.3	11.1	17.5
Feed flow rate (mL/min)	F	1.8	3.6	5.25
Inlet air temperature (°C)	T_{in}	75	150	220
Aspirator capacity (%)	A	80	90	100
Insulin concentration (mg/mL)	I	5	30	60

experiments were centre points. As the variation between the centre points is used to calculate the validity of the model in DoE, no replicates of the other experiments are necessary. At a later stage, the centre points were excluded from the training set and used as an external prediction set in the PLS models.

Morphology

The particle shape and surface morphology were investigated by scanning electron microscopy (SEM) using a Quanta 200 (FEI Company, Hillsboro, USA). The acceleration voltage was 10 kV and magnifications from ×1,000 to ×20,000 were used for all samples. The powder was sprinkled on a SEM stub, covered with adhesive carbon tape and sputter coated with gold prior to scanning. The signal is composed of secondary electrons.

Moisture Content

The moisture content in the powder samples was analysed by TGA with a TGA 7 (Perkin Elmer Inc., Waltham, USA) with nitrogen purging. The powder sample weighing approximately 2 mg was heated from 20°C to 250°C at a rate of 10°C/min. The weight loss observed between 20°C and 160°C was assigned to water evaporation from the powder and the weight change in per cent was defined as the moisture content of the powder. Weight losses occurring after 160°C were likely due to thermal decomposition of insulin.

Aerodynamic Particle Size

The aerodynamic particle size was determined using an Aerodynamic Particle Sizer Spectrometer 3321 equipped with a Small-Scale Powder Disperser (TSI Incorporated, Shoreview, MN, USA) used to generate the aerosol. The instrument employs a time of flight principle, measuring the velocity of the individual particles. The aerodynamic diameter was defined as the diameter of a spherical particle with the same velocity and behaviour as the analysed particle. The resulting particle size distribution was number-based and afterwards converted to a mass-based particle size distribution by the software provided with the instrument. A few milligrammes of spray-dried powder were placed on the turntable inside the small-scale powder disperser and introduced into the aerodynamic particle sizer by a Venturi aspirator. The flow rate and the rotation rate of the small-scale powder disperser were controlled to yield a particle concentration in the range of 0.3–3.0 mg/m^3 and analysis was continuously carried out for 20 s. It was assumed that the shear forces present in the small-scale powder disperser were sufficient to deagglomerate the spray-dried particles. In the following text, the aerodynamic particle size is given as the mass median aerodynamic diameter (MMAD).

Geometric Particle Size

The geometric particle size was analysed by laser diffraction with a Helos system (Sympatec GmbH, Clausthal-Zellerfeld, Germany). The powder was dispersed in isopropanol with Tween 20 and the optical density of the dispersion was adjusted to approximately 10% prior to measuring. The used wavelength was 632.8 nm. The particle size stated is the mass median diameter.

Near Infrared Spectroscopy and Multivariate Data Analysis

The near infrared (NIR) spectra were collected on a Bomem FTLA 2000 series FT-NIR spectrometer (Bomem, Quebec, Canada) in reflectance mode. NIR spectra were recorded through the bottom of the glass vials for each dried sample. Samples were rotated and measured again to decrease any possible effect of uneven distribution of powder. Samples were measured in the range of 8,000 to 4,000 cm^{-1} with a resolution of 8 cm^{-1} at ambient temperature. Each spectrum consisted of 32 scans. PLS models and calculations were computed using Simca-P v. 11.5 (Umetrics AB, Umeaa, Sweden). Spectral preprocessing was for some models applied prior to multivariate data analysis to reduce variation caused by unwanted variation and noise. Derivatives were applied to improve resolution of overlapping bands, while standard normal variate (SNV) transformation was used to reduce variation caused by physical characteristics (39–41). Based on previous experience, the PLS regression was performed on untreated spectra, standard normal variate spectra, first derivative and second derivate spectra (7). In all models, the spectra were centred prior to analysis regardless of the pretreatment method, while no other scaling (such as univariate scaling) was applied. Cross-validation was performed on all PLS models in addition with the validation plot addressing the uniqueness of the models. The cross-validation is performed with the standard settings of the software. The software divides the data set into seven random parts and performs parallel PLS models on the reduced data with one of the groups deleted. For every cycle, one part of the data set is removed and a model is built on the remaining six parts. The left out data are predicted from the model. This is repeated until all the data had been predicted. The predicted data were compared with original data and the sum of squared errors was calculated and converted into Q^2. For comparisons of models, the root mean square error of estimation (RMSEE) and cross-validation (RMSECV) were used together with goodness of fit (R^2) and prediction (Q^2). External validation was used where four centre points were excluded from the data set and used as prediction set. The root mean square error of prediction (RMSEP) for moisture content and

MMAD models was calculated based on the difference between the predicted and reference value for each sample in the prediction set.

RESULTS AND DISCUSSION

In DoE, several plausible models can be used for the investigation of a design space, all based on the desired detail of obtained knowledge. In the current investigation, screening was not necessary due to prior knowledge and an optimization design was applied to include both interaction and nonlinear behaviour of the factors. Thus, a central composite face-centred experimental design (CCF) was used to determine the parameters for the production of spray-dried powders with varying particle sizes and moisture contents, resulting in 31 production runs. A more detailed description of the experimental design is given in (24). All 31 spray-drying experiments produced white non-cohesive powders with distinct particles according to SEM analysis. Three distinct morphologies were observed for the spray-dried powders classified as spherical-shaped particles (type I), wrinkled particles (type II) and highly folded particles (type III) (Fig. 1) (24). The deposition of particles in the lungs is controlled by the aerodynamic particle size which is correlated to the geometric particle size, density of the particle and shape or morphology of the particle (42). The particle density is an important parameter, and particles with a large geometric particle size and low density have been designed for improved delivery to the lungs (20). The morphology of the particle is equally important and most particle shapes result in a lower aerodynamic particle size compared with a spherical particle. Thus, particles with a low density and non-spherical shape are preferred for pulmonary delivery, corresponding to the type III particles in this study.

The NIR spectra of several spray-dried insulin powder samples are shown in Fig. 2. The spectral region 7,000–5,600 cm^{-1} is assigned to overtones of the insulin molecule. The bands in the region 5,900–5,700 cm^{-1} are the first overtones of the C–H stretching and the band around 6,630 cm^{-1} is associated with the first overtone of the N–H stretching. The spectrum is dominated by combination bands in the 5,200–4,000 cm^{-1} region, similar to bands found for other proteins. Most of these bands have been tentatively assigned to combinations of amide I, amide II, amide III, amide A, amide B and C–H stretching bands (43,44). For the spray-dried insulin powders, two bands are observed around 6,900 and 5,150 cm^{-1} in the NIR spectra. These two bands originate from vibrations in the water molecule and the frequency depends on the environment and hydrogen bonding of the water molecules in the formulation (45). The band around 6,900 cm^{-1} corresponds to the first overtone of the OH stretching, $2\upsilon(OH)$ and the band around 5,150 cm^{-1} is associated with the combination band of the OH stretching and bending, $\upsilon(OH)+\delta(OH)$. These bands have previously been used to predict the water content in lyophilized and granulated samples (6–8,30,34,36).

Moisture Content

For the 31 experiments, the moisture content measured by loss of weight (TGA) was between 4% and 10%. NIR spectra of the spray-dried samples show that the water bands

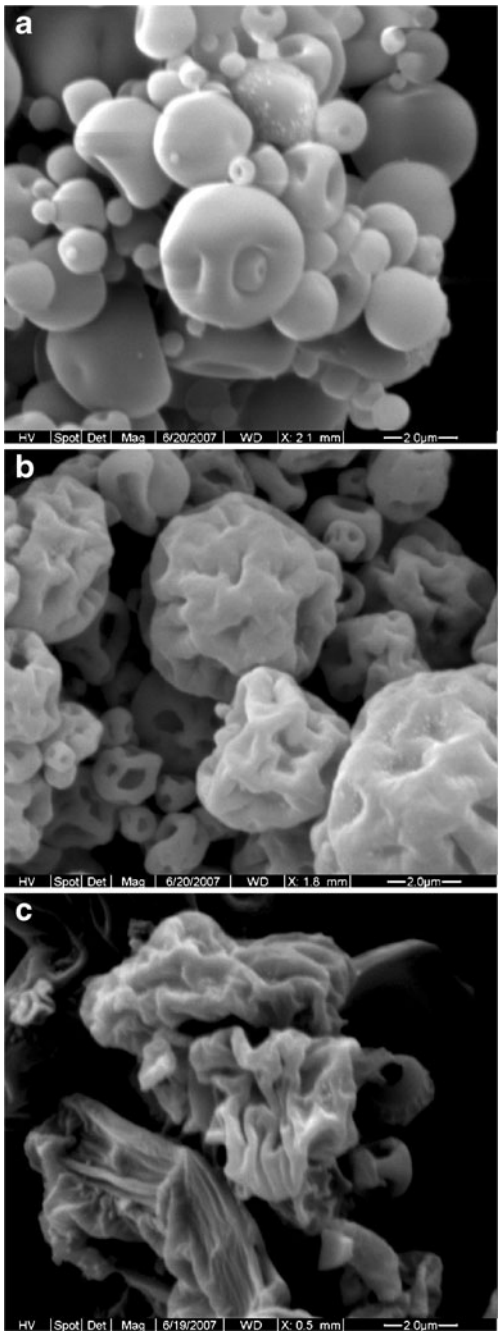

Fig. 1. Scanning electron microscopy pictures of spray-dried insulin particles illustrating the three different morphologies. **a** Morphology type I (*spherical*), **b** morphology type II (*wrinkled*) and **c** morphology type III (*highly folded*)

at 6,900 and 5,150 cm^{-1} change in intensity with varying moisture content (Fig. 2a). An increase in moisture content results in an increase in intensity in these two bands and a baseline variation. Bands originating from insulin overlap with the water bands making it difficult to use the band intensity for direct quantification. The band at 6,900 cm^{-1} primarily overlaps with the N–H overtone bands and the band at 5,150 cm^{-1} overlaps with combination bands from the insulin molecule. Different pre-treatment methods have previously been used in combination with NIR spectroscopy to enhance the chemical information in the spectral data set. A commonly

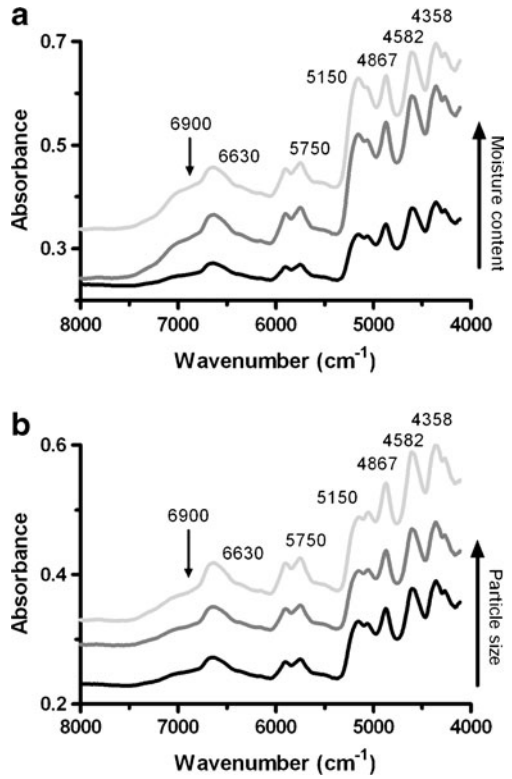

Fig. 2. NIR spectra of spray-dried insulin. **a** Spectra of powders with different moisture content: 4.8% (*black*), 7.1% (*grey*) and 9.2% (*light grey*). **b** Spectra of powders with different aerodynamic particle sizes: 1.38 μm (*black*), 3.13 μm (*grey*) and 4.12 μm (*light grey*)

used method is to transform the spectra, eliminating the physical information in the spectral data set. First derivative, second derivative, and standard normal variate (SNV) transformations have all been used with success when correlating NIR spectra with moisture content (7,8,34). In this study, all three pre-treatment methods were tested, in addition to the untreated data set, in the PLS analysis. An overview of the four cross-validated PLS models is given in Table II. Restricting the included wavenumbers to specific ranges was investigated for the spectral data set, but none were found to improve the quality of the model based on the entire spectral range (data not shown).

The untreated spectral data set showed a low correlation between the variation in the NIR spectra and the moisture content. This becomes evident as the first PLS component utilizes a large portion (92.5%) of the NIR spectra to explain a minor portion (21.5%) of the moisture content. This is due to the fact that the main variation in untreated data often is a baseline offset. This offset can be related to the water content, but needs a larger proportion of the spectral variance to obtain a correlation to the moisture content than specific water absorption bands. In contrast, the first PLS components in the three models based on pre-treated spectra correlate the majority of the variation in the spectra (73.2% for first derivative, 61.4% for second derivative and 57.0% for SNV) to the majority of the variation in the moisture content (85.5% for first derivative, 68.4% for second derivative and 93.3% for SNV). The PLS models based on the first and second derivative performed slightly better compared with the model based on the untreated absorbance data set, with one less PLS component due to removal of most of the physical variation found in the first PLS component of the untreated absorbance data set (Table II).

SNV correction resulted in a simple PLS model with only one component and a linear correlation between NIR spectra and moisture content (Fig. 3a). The loading plot for the PLS component of the model based on the SNV treated data set shows two significant features corresponding to the two bands originating from the water molecule in the NIR spectrum (Fig. 3b). At low wavenumbers, features of the insulin spectrum are present in the loading plot and are negatively correlated with the moisture content. Thus, the SNV model mainly reflects the variation in the moisture content from the two water bands and the combination bands originating from the insulin molecule below 5,000 cm^{-1}.

All models predict the moisture content with an error similar to the reference method (0.4%) and with a RMSECV and RMSEP in the same range as previously published models developed for lyophilised mannitol and trehalose (0.42%) (7) and granulation of lactose (0.59%) (8). The actual and predicted moisture content of the four samples (centre points) in the prediction data set were tested with two-way analysis of variance (ANOVA). There was no significant difference between the predicted moisture content of the four PLS models and the actual measured moisture content by TGA (Fig. 3c). However, the four samples had a significantly different moisture content indicating sample to sample variation in the spray-drying process. In conclusion, the overlapping features of insulin with the bands originating from the water molecules in the NIR spectrum and the spray-drying method do not influence the prediction of the moisture content by the PLS models.

Table II. PLS Model Overview of Moisture Content

Models				
Pre-treatment	None	SNV	1st derivative	2nd derivative
Wavenumber (cm^{-1})	8,000–4,000	8,000–4,000	8,000–4,000	8,000–4,000
PLS components	3	1	2	2
RMSEE (%)	0.39	0.36	0.36	0.35
R^2	0.93	0.93	0.94	0.94
RMSECV (%)	0.44	0.39	0.37	0.35
Q^2	0.90	0.92	0.92	0.92
RMSEP (%)	0.46	0.44	0.48	0.39

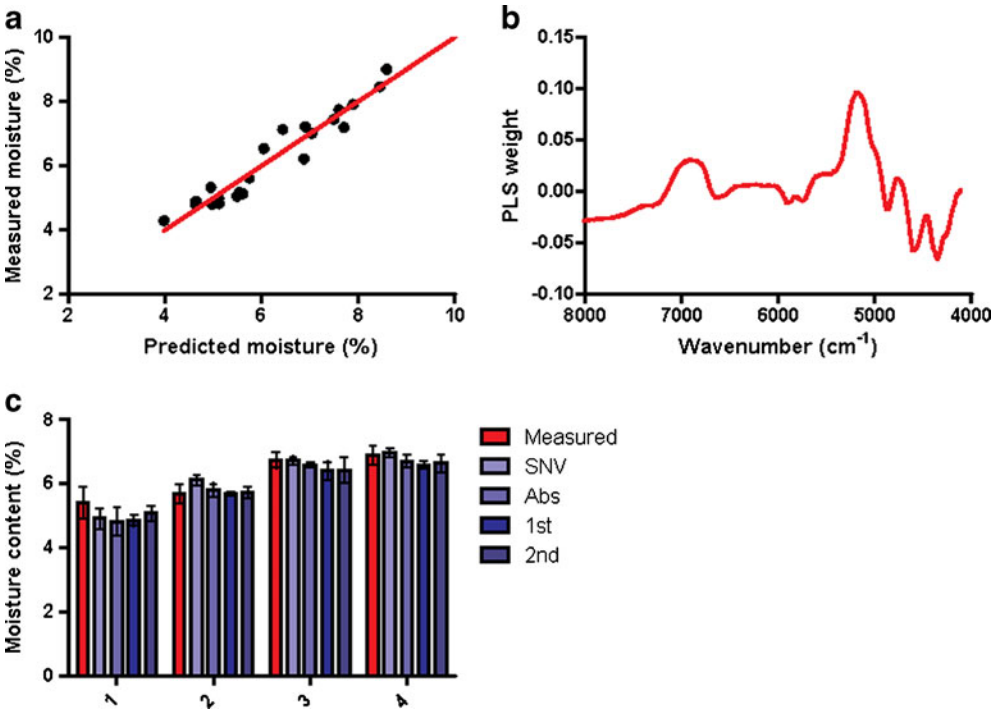

Fig. 3. PLS model of moisture content based on SNV treated spectra. **a** Correlation between moisture content obtained by PLS model and measured by TGA. **b** Loading plot of the first PLS component. **c** Measured and predicted moisture content for the four centre points used as prediction set

Aerodynamic Particle Size

For the spray-dried insulin, not only the moisture content, but also the particle size of the spray-dried powders is an important variable. The aerodynamic particle size was measured with a time of flight (TOF) principle and yielded MMAD in the range of 1.38–5.81 μm for the investigated process design space. This range of aerodynamic particle sizes reflects the optimal size range for particles intended for pulmonary delivery (17).

The effects of particle size on the NIR absorbance spectra can be observed in Fig. 2b, where an increasing particle size results in an increase in absorbance due to scattering effects of the particles for three representative samples. Scattering is not only dependent on the particle size, but also other particle characteristics such as density, shape, refractive index and uniformity have a significant impact. In order to evaluate NIR as a possible technique for measuring the particle size of spray-dried powders in the size range suitable for pulmonary delivery, the measured MMAD was correlated with the NIR spectra. An overview of the cross-validated PLS models of the aerodynamic particle size is given in Table III, and measured *versus* predicted MMAD is given in Fig. 4a for the untreated NIR spectra. Three PLS components were needed to correlate the untreated NIR spectra (Fig. 4b), the first derivative and the second derivative pre-treated spectra with the aerodynamic particle size. In the loading plot for the PLS model based on the untreated data, the first two PLS components resemble the NIR spectra of insulin with different degrees of baseline offset, while the dominant features for the third PLS component are the two bands originating from water (Fig. 4b). The first two PLS components correlate the main variation in the spectral data set (80.4% and 19.1%, respectively) with the main variation in aerodynamic particle size (24.0% and 49.0%, respectively). Interestingly, the first PLS component is positive at wavenumbers below 7,000 cm^{-1} and the second PLS component is positive at wavenumbers below 5,200 cm^{-1}. This shows that an increase in particle size results in an increase in scattering intensity at low wavenumbers but not at high wavenumbers. This has been observed before for particles below 20 μm and is due to a decrease in direct backscatter and increase in path length for

Table III. PLS Model Overview of Aerodynamic Particle Size

Models			
Pre-treatment	None	1st derivative	2nd derivative
Wavenumber range (cm^{-1})	8,000–4,000	8,000–4,000	8,000–4,000
PLS components	3	3	3
RMSEE (μm)	0.47	0.43	0.44
R^2	0.82	0.85	0.84
RMSECV (μm)	0.53	0.48	0.53
Q^2	0.77	0.78	0.72
RMSEP (μm)	0.27	0.29	0.44

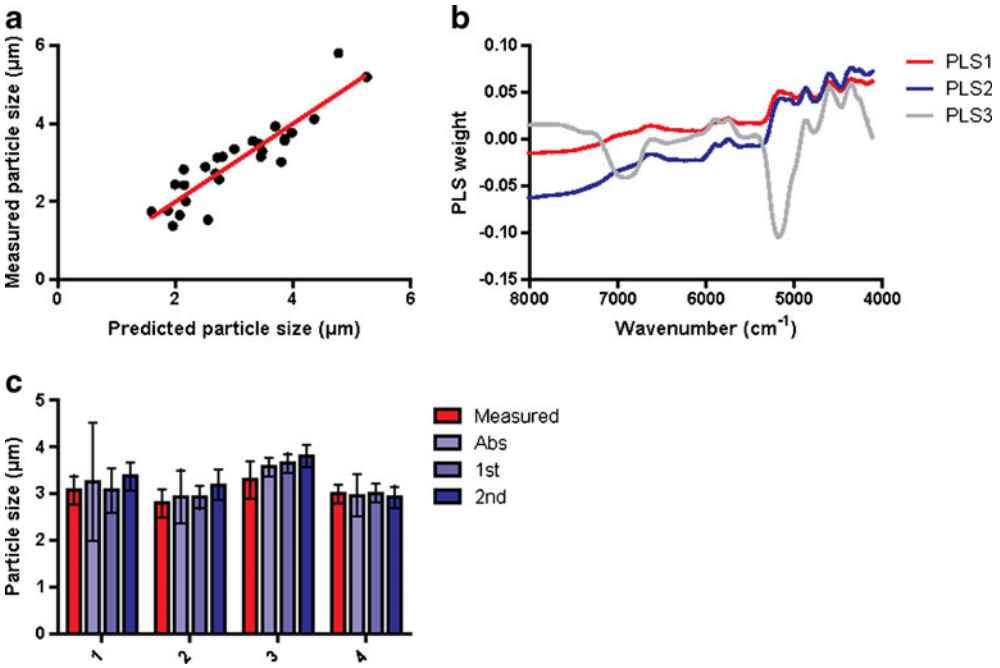

Fig. 4. PLS model of aerodynamic particle size based on untreated spectra. **a** Correlation between aerodynamic particle size obtained by PLS model and measured by TOF principle. **b** Loading plot of the PLS components: PLS 1, PLS 2 and PLS 3. **c** Measured and predicted aerodynamic particle size for the four centre points used as prediction set

small particles at larger wavelengths (46). The correlation between baseline offset and the aerodynamic particle size implies that SNV transformation cannot be used since this transformation reduces the baseline offset. The last PLS component, based on the characteristic water bands, indicates that smaller particles have a higher moisture content and moisture accounts for 9.5% of the aerodynamic particle size variation.

While the first PLS component describes 24.0% of the variation in the aerodynamic particle size, the majority of the variation is not accounted for, which indicates that other physical particle characteristics contribute to the variation in the spectra. In order to decrease the effect of these physical parameters, first and second derivative transformations are tested as pre-treatment methods to reduce the amount of nonsignificant variation in the spectral data set compared with the untreated NIR spectra. For the model based on first derivative spectra, the first PLS component correlates 73.6% of the variation in the spectral data set with 59.2% of the variation in the aerodynamic particle size, whereas for the model based on second derivative spectra, the first PLS component uses 68.2% of the spectral variation to explain 67.8% of the aerodynamic particle size variation. However, none of the derivative models perform better than the model based on the untreated spectra in terms of RMSEE, RMSECV and RMSEP.

The actual and predicted MMAD of the four samples (centre points) in the prediction data set were tested with two-way ANOVA. There was no significant difference between the predictions of the four PLS models and the actual measured aerodynamic particle size by TOF (Fig. 4c). In conclusion, NIR spectroscopy in combination with PLS analysis could be an alternative to measuring the aerodynamic particle size by TOF.

Influence of Particle Morphology on Aerodynamic Particle Size

To further evaluate the effect of particle characteristics on the NIR spectra and the ability to predict the particle size, the 31 experiments were divided into three groups according to morphology (Fig. 1) and new PLS models were computed. Models were made for untreated spectra, first derivative and second derivative pre-treated spectra. The model based on the untreated spectra performed slightly better compared to the models based on derivative spectra for RMSEE and RMSECV (data not shown). For all three morphologies, four PLS components are required to correlate the untreated spectra with the aerodynamic particle size (Table IV).

The PLS model based on type I morphology (spherical shaped) predicts the aerodynamic particle size (Fig. 5a) with a low RMSECV (0.22 µm) and high predictability (Q^2 is 0.97). The aerodynamic particle size range for particles with type I morphology is from 2.42 to 5.81 µm. Particles with type II morphology are still distinct particles, but have a more wrinkled and irregular-shaped surface. The aerodynamic particle size range is from 2.57 to 4.12 µm and the model performs equally well as the PLS model for type I morphology (RMSECV is 0.16 µm and Q^2 is 0.88). Type III morphology encompasses particles with a highly folded structure and a clear distinction between particles cannot always be assigned. In general, the PLS model based on particles with a type III morphology performs worse compared with the other morphologies (RMSECV is 0.44 µm and Q^2 is 0.69).

As discussed above, reasonably predictive models can be obtained for type I and type II morphologies, whereas particle diameter for particles with type III morphology are not easily predicted. Thus, morphology clearly matters for scattering of the NIR spectra and the subsequent prediction of the particle

Table IV. PLS Models of Aerodynamic Particle Size Based on Morphology

Morphology type	I	II	III
Wavenumber range (cm^{-1})	8,000–4,000	8,000–4,000	8,000–4,000
No of observations	8	13	10
Particle size range (μm)	2.42–5.81	2.57–4.12	1.38–3.35
Pre-treatment	None	None	None
PLS components	4	4	4
RMSEE (μm)	0.11	0.13	0.32
R^2	0.99	0.94	0.88
RMSECV (μm)	0.22	0.16	0.44
Q^2	0.97	0.88	0.69

I spherical-shaped particles, *II* wrinkled particles, *III* highly folded shaped particles

size of the spray-dried particles. The influence of morphology on the PLS models can be explained by the differences in the analytical principle used for NIR and aerodynamic particle size. The PLS models based on NIR spectra are founded on differences in light scattering of particles, whereas aerodynamic particle size is measured by TOF independent of particle scattering. The difference is clarified when looking at the geometric particle size measured by laser diffraction. It can be seen in Fig. 5b that even with rather similar geometric particle sizes, large differences in aerodynamic particle sizes are found due to different morphology and density. Especially for type III and to some extent type II morphology, a low correlation is observed between aerodynamic and geometric particle size. For regulatory approval, the aerodynamic particle size has to be measured with multistage cascade impactors providing a direct link between mass of active pharmaceutical ingredient and aerodynamic particle size; this direct link is not obtained with TOF or NIR measurements. However, both TOF and NIR are significantly faster and more suitable for continuous monitoring of aerodynamic particle size than multistage cascade impactors. For TOF measurements, the sample is removed from the spray-drying process. Although our measurements were performed at-line through the bottom of a glass vial, the application of an instrumentation with a fibre optic probe, NIR measurements can in principle be done directly on a glass collection vessel, thus making it an excellent choice for in-line analysis of the aerodynamic particle size for formulations intended for pulmonary delivery.

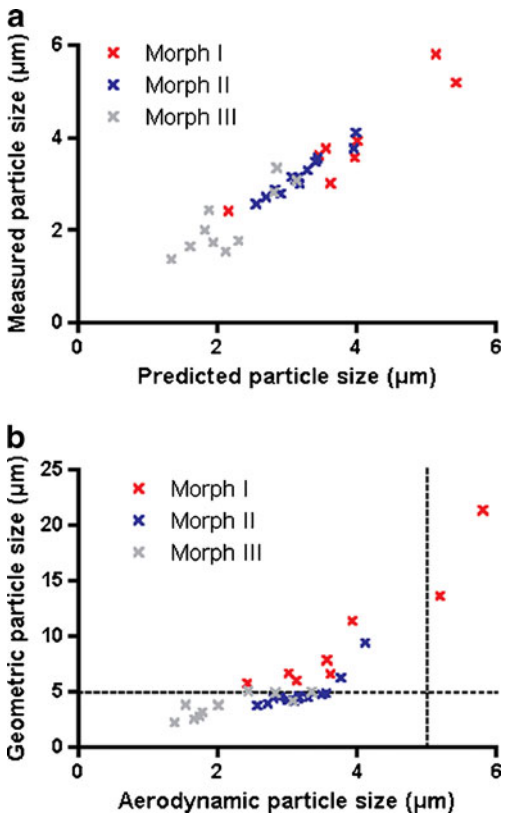

Fig. 5. **a** PLS model of aerodynamic particle size based on untreated data categorized by morphology. **b** Geometric particles size plotted as a function of aerodynamic particle

CONCLUSION

In product quality monitoring, moisture content and particle size are critical quality attributes for spray-dried powders. The NIR models developed in this study can be used to monitor the moisture content of the spray-dried insulin, based on the chemical information of the water molecules in the NIR spectrum of the spray-dried powders. All models yielded good fits, good predictions and RMSEPs comparable with the reference method (TGA) but the SNV model is recommended due to a lower number of PLS components.

The NIR spectra also yielded useful information on the particle size and could be correlated to results obtained from TOF. The morphology of the spray-dried particles had a significant impact on the models; especially for highly folded particles it was difficult to build robust models, while good models were achieved for particles with a more uniform morphology. Multivariate analysis of the NIR spectra showed a good prediction of the aerodynamic particle size. Thus, NIR was successfully applied for at-line process analysis, and can in principle be used for in-line process analysis at the glass collection vessel, in order to monitor both particle size and moisture content of a spray-drying process.

ACKNOWLEDGMENTS

This work was funded by the Drug Research Academy and Novo Nordisk. The authors would like to thank Novo Nordisk for providing the insulin.

REFERENCES

1. International Conference on Harmonisation (ICH). Quality guidelines: Q8-10. Geneva: ICH; 2005.
2. European Medicines Agency (EMA). Note for guidance on pharmaceutical development (EMEA/CHMP/167068/2004). London: EMA; 2006.
3. Food and Drug Administration (FDA). Guidance for industry. PAT—a framework for innovative pharmaceutical development, manufacturing and quality assurance. Rockville: FDA; 2004.
4. Rathore AS, Winkle H. Quality by design for biopharmaceuticals. Nat Biotechnol. 2009;27(1):26–34.
5. Rathore AS. Roadmap for implementation of quality by design (QbD) for biotechnology products. Trends Biotechnol. 2009;27 (9):546–53.
6. Blanco M, Cueva-Mestanza R, Peguero A. Controlling individual steps in the production process of paracetamol tablets by use of NIR spectroscopy. J Pharm Biomed Anal. 2010;51(4):797–804.
7. Grohganz H, Fonteyne M, Skibsted E, Falck T, Palmqvist B, Rantanen J. Role of excipients in the quantification of water in lyophilised mixtures using NIR spectroscopy. J Pharm Biomed Anal. 2009;49(4):901–7.
8. Nieuwmeyer FJ, Damen M, Gerich A, Rusmini F, van der Voort Maarschalk K, Vromans H. Granule characterization during fluid bed drying by development of a near infrared method to determine water content and median granule size. Pharm Res. 2007;24 (10):1854–61.
9. Reich G. Near-infrared spectroscopy and imaging: basic principles and pharmaceutical applications. Adv Drug Deliv Rev. 2005;57(8):1109–43.
10. Teixeira AP, Oliveira R, Alves PM, Carrondo MJ. Advances in online monitoring and control of mammalian cell cultures: supporting the PAT initiative. Biotechnol Adv. 2009;27(6):726–32.
11. Wang W. Instability, stabilization, and formulation of liquid protein pharmaceuticals. Int J Pharm. 1999;185(2):129–88.
12. Wang W. Lyophilization and development of solid protein pharmaceuticals. Int J Pharm. 2000;203(1–2):1–60.
13. Carpenter JF, Pikal MJ, Chang BS, Randolph TW. Rational design of stable lyophilized protein formulations: some practical advice. Pharm Res. 1997;14(8):969–75.
14. Chang LL, Pikal MJ. Mechanisms of protein stabilization in the solid state. J Pharm Sci. 2009;98(9):2886–908.
15. Allison SD, Chang B, Randolph TW, Carpenter JF. Hydrogen bonding between sugar and protein is responsible for inhibition of dehydration-induced protein unfolding. Arch Biochem Biophys. 1999;365(2):289–98.
16. Carpenter JF, Crowe JH. An infrared spectroscopic study of the interactions of carbohydrates with dried proteins. Biochemistry. 1989;28(9):3916–22.
17. Patton JS, Byron PR. Inhaling medicines: delivering drugs to the body through the lungs. Nat Rev Drug Discov. 2007;6(1):67–74.
18. Shoyele SA, Cawthorne S. Particle engineering techniques for inhaled biopharmaceuticals. Adv Drug Deliv Rev. 2006;58(9–10):1009–29.
19. Vehring R. Pharmaceutical particle engineering via spray drying. Pharm Res. 2008;25(5):999–1022.
20. Chow AH, Tong HH, Chattopadhyay P, Shekunov BY. Particle engineering for pulmonary drug delivery. Pharm Res. 2007;24(3):411–37.
21. Vega C, Roos YH. Invited review: spray-dried dairy and dairy-like emulsions compositional considerations. J Dairy Sci. 2006;89 (2):383–401.
22. Mack GS. Pfizer dumps Exubera. Nat Biotechnol. 2007;25 (12):1331–2.
23. Maltesen MJ, van de Weert M. Drying methods for protein pharmaceuticals. Drug Discov Today Technol. 2008;5(2–3):e81–8.
24. Maltesen MJ, Bjerregaard S, Hovgaard L, Havelund S, van de Weert M. Quality by design—spray drying of insulin intended for inhalation. Eur J Pharm Biopharm. 2008;70(3):828–38.
25. Stahl K, Claesson M, Lilliehorn P, Linden H, Backstrom K. The effect of process variables on the degradation and physical properties of spray dried insulin intended for inhalation. Int J Pharm. 2002;233(1–2):227–37.
26. Burgess DJ, Duffy E, Etzler F, Hickey AJ. Particle size analysis: AAPS workshop report, cosponsored by the Food and Drug Administration and the United States Pharmacopeia. AAPS J. 2004;6(3):e20.
27. Shekunov BY, Chattopadhyay P, Tong HH, Chow AH. Particle size analysis in pharmaceutics: principles, methods and applications. Pharm Res. 2007;24(2):203–27.
28. O'Neil AJ, Jee RD, Moffat AC. Measurement of the percentage volume particle size distribution of powdered microcrystalline cellulose using reflectance near-infrared spectroscopy. Analyst. 2003;128(11):1326–30.
29. Pasikatan MC, Steele JL, Spillman CK, Haque E. Near infrared reflectance spectroscopy for online particle size analysis of powders and ground materials. J Near Infrared Spectrosc. 2001;9:153–64.
30. Alcala M, Blanco M, Bautista M, Gonzalez JM. On-line monitoring of a granulation process by NIR spectroscopy. J Pharm Sci. 2010;99(1):336–45.
31. Frake P, Gill I, Luscombe CN, Rudd DR, Waterhouse J, Jayasooriya UA. Near-infrared mass median particle size determination of lactose monohydrate, evaluating several chemometric approaches. Analyst. 1998;123(10):2043–6.
32. O'Neil AJ, Jee RD, Moffat AC. The application of multiple linear regression to the measurement of the median particle size of drugs and pharmaceutical excipients by near-infrared spectroscopy. Analyst. 1998;123(11):2297–302.
33. Baldinger A, Clerdent L, Rantanen J, Yang M, Grohganz H. Quality by design approach in the optimization of the spray-drying process. Pharm Dev Technol. 2011. doi:10.3109/10837450.2010.550623.
34. Cao W, Mao C, Chen W, Lin H, Krishnan S, Cauchon N. Differentiation and quantitative determination of surface and hydrate water in lyophilized mannitol using NIR spectroscopy. J Pharm Sci. 2006;95(9):2077–86.
35. Zheng Y, Lai X, Bruun SW, Ipsen H, Larsen JN, Lowenstein H, *et al.* Determination of moisture content of lyophilized allergen vaccines by NIR spectroscopy. J Pharm Biomed Anal. 2008;46(3):592–6.
36. Zhou GX, Ge Z, Dorwart J, Izzo B, Kukura J, Bicker G, *et al.* Determination and differentiation of surface and bound water in drug substances by near infrared spectroscopy. J Pharm Sci. 2003;92(5):1058–65.
37. Maltesen MJ, Bjerregaard S, Hovgaard L, Havelund S, van de Weert M, Grohganz H. Multivariate analysis of phenol in freeze-dried and spray-dried insulin formulations by NIR and FTIR. AAPS PharmSciTech. 2011;12(2):627–36.
38. Kaarsholm NC, Havelund S, Hougaard P. Ionization behavior of native and mutant insulins: pK perturbation of B13-Glu in aggregated species. Arch Biochem Biophys. 1990;283(2):496–502.
39. Barnes RJ, Dhanoa MS, Lister SJ. Standard normal variate transformation and de-trading of near-infrared diffuse reflectance specrta. Appl Spectrosc. 1989;43(5):772–7.
40. Norris KH, Williams PC. Optimization of mathematical treatments of raw near-inrared signal in the measurement of protein in hard red spring wheat. 1. Influence of particle size. Cereal Chem. 1984;61(2):158–65.
41. Rinnan A, van den Berg F, Engelsen SB. Review of the most common pre-processing techniques for near-infrared spectra. TrAC. 2009;28(10):1201–22.
42. Crowder TM, Rosati JA, Schroeter JD, Hickey AJ, Martonen TB. Fundamental effects of particle morphology on lung delivery: predictions of Stokes' law and the particular relevance to dry powder inhaler formulation and development. Pharm Res. 2002;19(3):239–45.
43. Bai SJ, Nayar R, Carpenter JF, Manning MC. Noninvasive determination of protein conformation in the solid state using near infrared (NIR) spectroscopy. J Pharm Sci. 2005;94(9):2030–8.
44. Bruun SW, Sondergaard I, Jacobsen S. Analysis of protein structures and interactions in complex food by near-infrared spectroscopy. 1. Gluten powder. J Agric Food Chem. 2007;55(18):7234–43.
45. Miller CE. Chemical principles of near infrared technology. In: Williams P, Norris K, editors. Near infrared technology in the agricultural and food industries. 2nd ed. Saint Paul: American Association of Cereal Chemists; 2012. p. 19–37.
46. Bittner LK, Heigl N, Petter CH, Noisternig MF, Griesser UJ, Bonn GK, *et al.* Near-infrared reflection spectroscopy (NIRS) as a successful tool for simultaneous identification and particle size determination of amoxicillin trihydrate. J Pharm Biomed Anal. 2011;54(5):1059–64.